



## OPEN ACCESS

## EDITED BY

Tiziana Rancati,  
National Cancer Institute Foundation  
(IRCCS), Italy

## REVIEWED BY

Alessandro Cicchetti,  
National Cancer Institute Foundation  
(IRCCS), Italy  
Serena Monti,  
National Research Council (CNR), Italy

## \*CORRESPONDENCE

Wonmo Sung

✉ wsung@catholic.ac.kr

Jee Suk Chang

✉ changjeesuk@yuhs.ac

RECEIVED 05 October 2022

ACCEPTED 10 May 2023

PUBLISHED 29 May 2023

## CITATION

Shin Y, Chang JS, Kim Y, Shin SJ, Kim J,  
Kim TH, Liu M, Olson R, Kim JS and  
Sung W (2023) Mathematical prediction  
with pretreatment growth rate of  
metastatic cancer on outcomes:  
implications for the characterization of  
oligometastatic disease.  
*Front. Oncol.* 13:1061881.  
doi: 10.3389/fonc.2023.1061881

## COPYRIGHT

© 2023 Shin, Chang, Kim, Shin, Kim, Kim, Liu,  
Olson, Kim and Sung. This is an open-access  
article distributed under the terms of the  
[Creative Commons Attribution License  
\(CC BY\)](https://creativecommons.org/licenses/by/4.0/). The use, distribution or  
reproduction in other forums is permitted,  
provided the original author(s) and the  
copyright owner(s) are credited and that  
the original publication in this journal is  
cited, in accordance with accepted  
academic practice. No use, distribution or  
reproduction is permitted which does not  
comply with these terms.

# Mathematical prediction with pretreatment growth rate of metastatic cancer on outcomes: implications for the characterization of oligometastatic disease

Yerim Shin<sup>1</sup>, Jee Suk Chang<sup>2,3\*</sup>, Yeseul Kim<sup>1</sup>, Sang Joon Shin<sup>4</sup>,  
Jina Kim<sup>2</sup>, Tae Hyung Kim<sup>5</sup>, Mitchell Liu<sup>3</sup>, Robert Olson<sup>6</sup>,  
Jin Sung Kim<sup>7</sup> and Wonmo Sung<sup>1\*</sup>

<sup>1</sup>Department of Biomedical Engineering and of Biomedicine & Health Sciences, College of Medicine, The Catholic University of Korea, Seoul, Republic of Korea, <sup>2</sup>Department of Radiation Oncology, Yonsei University College of Medicine, Seoul, Republic of Korea, <sup>3</sup>BC Cancer - Vancouver Centre, Vancouver, BC, Canada, <sup>4</sup>Division of Medical Oncology, Department of Internal Medicine, Yonsei University College of Medicine, Seoul, Republic of Korea, <sup>5</sup>Department of Radiation Oncology, Nowon Eulji Medical Center, Eulji University School of Medicine, Seoul, Republic of Korea, <sup>6</sup>BC Cancer, Centre for the North, Prince George, BC, Canada, <sup>7</sup>Department of Radiation Oncology, Yonsei Cancer Center, Heavy Ion Therapy Research Institute, Yonsei University College of Medicine, Seoul, Republic of Korea

**Background:** Oligometastatic disease (OMD) represents an indolent cancer status characterized by slow tumor growth and limited metastatic potential. The use of local therapy in the management of the condition continues to rise. This study aimed to investigate the advantage of pretreatment tumor growth rate in addition to baseline disease burden in characterizing OMDs, generally defined by the presence of  $\leq 5$  metastatic lesions.

**Methods:** The study included patients with metastatic melanoma treated with pembrolizumab. Gross tumor volume of all metastases was contoured on imaging before (TP<sub>-1</sub>) and at the initiation of pembrolizumab (TP<sub>0</sub>). Pretreatment tumor growth rate was calculated by an exponential ordinary differential equation model using the sum of tumor volumes at TP<sub>-1</sub> and TP<sub>0</sub> and the time interval between TP<sub>-1</sub> and TP<sub>0</sub>. Patients were divided into interquartile groups based on pretreatment growth rate. Overall survival, progression-free survival, and subsequent progression-free survival were the study outcomes.

**Results:** At baseline, median cumulative volume and number of metastases were 28.4 cc (range, 0.4-1194.8 cc) and 7 (range, 1-73), respectively. The median interval between TP<sub>-1</sub> and TP<sub>0</sub> was -90 days and pretreatment tumor growth rate ( $\times 10^{-2}$  days<sup>-1</sup>) was median 4.71 (range -0.62 to 44.1). The slow-paced group (pretreatment tumor growth rate  $\leq 7.6 \times 10^{-2}$  days<sup>-1</sup>, the upper quartile) had a significantly higher overall survival rate, progression-free survival, and subsequent progression-free survival compared to those of the fast-paced

group (pretreatment tumor growth rate  $> 7.6 \times 10^{-2} \text{ days}^{-1}$ ). Notably, these differences were prominent in the subgroup with  $>5$  metastases.

**Conclusion:** Pretreatment tumor growth rate is a novel prognostic metric associated with overall survival, progression-free survival, and subsequent progression-free survival among metastatic melanoma patients, especially patients with  $>5$  metastases. Future prospective studies should validate the advantage of disease growth rate plus disease burden in better defining OMDs.

#### KEYWORDS

immune checkpoint inhibitor, melanoma, mathematical modeling, oligometastasis, tumor growth rate

## 1 Introduction

Metastatic cancer has long been considered an incurable disease (1). However, in 1995, Hellman and Weichselbaum first proposed the oligometastatic disease (OMD) concept, suggesting that biologically limited small number of bundles or slowly progressing metastatic cancers could be curable (2). In addition, studies on ablation of gross metastatic tumors using stereotactic ablative radiotherapy (SABR) or surgery in patients with OMD from various histology has shown an improvement in survival outcomes; however, phase III trials remain pending in these studies (3, 4).

Since there are no biomarkers to define OMD, clinical trials have used either five or three metastatic lesions on imaging as the cutoff (5). Previous trials involving 1–3 or 1–5 metastases (6) have reported a sizable risk of rapid or widespread metastatic progression following SABR as being characteristic of OMD, thus raising a valid concern on the clinical application of SABR for OMD treatment in real-world practice. Pretreatment baseline tumor burden is widely acknowledged as an important indicator for cancer therapy and helps distinguish OMDs from polymetastatic diseases (7, 8). In the same context, randomized clinical trials testing new drugs against cancer used the baseline tumor burden as a stratification factor (7).

The present study was designed to determine whether OMD can be clinically defined based on the pretreatment growth rate of metastatic tumors. Using a cohort of metastatic melanoma patients treated with an immune checkpoint inhibitor (ICB), we developed a mathematical model with a simple exponential ordinary differential equation (ODE) to determine tumor growth rate of total disease burden prior to ICB administration, and thereafter, determine the effect of tumor growth rate on patient outcomes. Advancements in the methodological assessment of tumor growth may serve as a prognostic tool for per-patient response to cancer therapy.

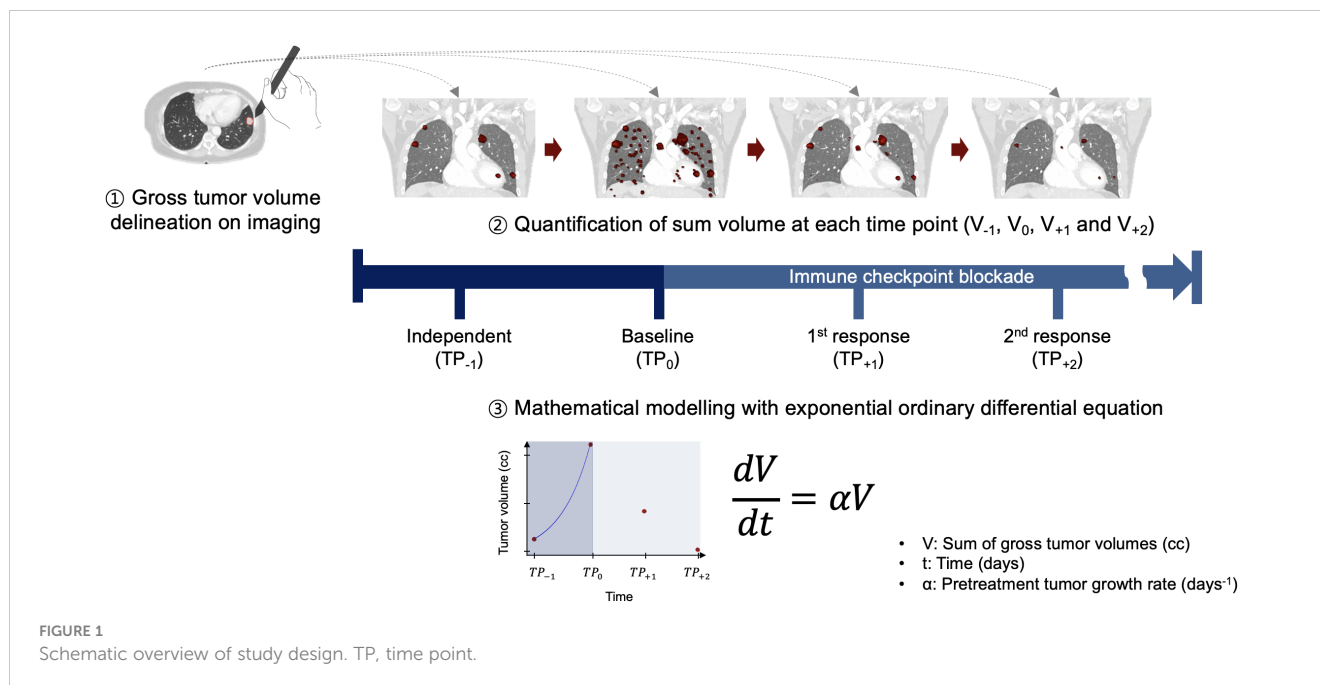
## 2 Materials and methods

### 2.1 Study design

This study was approved by the Institutional Review Board (4-2021-1683) of Severance Hospital, Seoul, Republic of Korea, and the requirement for patient informed consent was waived because of the study's retrospective design. We identified 86 patients with metastatic malignant melanoma who were treated with pembrolizumab monotherapy at a single center between 2015 and 2020. The patient's demographic information, clinical and tumor characteristics, time interval between the time of ICB treatment start (baseline) and pretreatment time point (TP<sub>-1</sub>), response to ICB treatment, and follow-up status were from a database (Figure 1). Patient data and tumor characteristics are summarized in Table 1. A separate study was conducted using the same study cohort to compare the prognostic value of a cumulative 3-dimensional (3D) volume of all metastases and counting the total number of metastases as a surrogate for the disease burden (8).

### 2.2 Study cohort

In this study cohort, patients with new tumor recurrence or metastatic tumor after prior treatment were treated with pembrolizumab, an anti-programmed cell death-1 antibody, monotherapy. Basic administration protocol was intravenous injection of 2 mg/kg doses every 2 or 3 weeks. Drug administration continued until disease progression or the 36<sup>th</sup> cycle, whichever came first. Baseline workup consisted of pathologic confirmation and computed tomography (CT) imaging of the chest and abdomen-pelvic area as well as the neck or upper/lower extremities, if necessary. When CT images showed equivocal findings, magnetic resonance imaging (MRI) was performed. In addition, brain MRIs to evaluate intracranial disease were



performed when patients complained of neurologic symptoms or at physicians' discretion if the patient was asymptomatic. Positron emission tomography-computed tomography (PET-CT) scan was performed in most patients to evaluate the extent and severity of any systemic disease. In brain metastasis, stereotactic radiosurgery and/or external beam radiotherapy (RT) was administered after a multidisciplinary discussion for intracranial diseases. Patients presenting with bleeding, pain, or mass effect were administered a local palliative RT to treat the symptom-causing lesion. Regular follow-up involving CT imaging of the chest, abdomen-pelvic area, and other areas, if necessary, were performed every three cycles of pembrolizumab administration.

### 2.3 Volumetric assessment

For quantitative assessment, board-certified radiation oncologists delineated the gross tumor volume of all metastatic lesions that appeared on available CT, PET-CT, and/or MRI (a) at the time of pembrolizumab initiation (baseline,  $TP_0$ ) and (b) independent from any clinical intervention ( $TP_{-1}$ ) using the MIM contouring tool (MIM Software Inc., version 7.1.7, Cleveland, OH, USA). Axial cut images with slice thickness  $\leq 3$  mm were used for tumor delineation, and multi-modality fusion was performed to accurately assess the extent and severity of the tumor. The total volume of all metastatic lesions from the two different time points were calculated. In patients who initially presented with metastatic melanoma at  $TP_0$  ( $n = 44$ ), we assumed the  $TP_{-1}$  status as the tumor volume of 0.1 cc 90 days prior to the baseline, considering that patients with melanoma typically undergo follow-ups involving conventional imaging, such as chest and abdominal CT scans every 3 months. To evaluate the initial volumetric change

following ICB administration, gross tumor volume was delineated on imaging at the time of first response evaluation 3 or 4 cycles after ICB administration ( $TP_{+1}$ ) and second response evaluation 6 or 7 cycles after ICB administration ( $TP_{+2}$ ). The total volume was calculated for comparison with the baseline ( $TP_0$ ) sum volume.

### 2.4 Mathematical model

Patient tumor growth rate was calculated by a well-known exponential ordinary differential function (Equation 1).

$$\frac{dV}{dt} = \alpha V \quad \text{Equation 1}$$

where  $V$  is the total tumor volume and  $\alpha$  is the tumor growth rate constant.

The Python `curve_fit` function and SciPy `odeint` function in addition to fitting the best-fit exponential ODE curve between the data measured at  $TP_{-1}$  and  $TP_0$  were used to obtain an optimal fitting solution for patient's pretreatment tumor growth rate ( $\alpha$ ). Considering that other ODE models require the determination of other parameters such as growth limit and natural death of cells, the application of the exponential model in determining tumor growth rate is relatively easy. Since our study is mainly focused on intrinsic tumor growth rate, we contemplated on using only an exponential model for the analysis. However, to compare other mathematical models, according to Murphy et al. (9), six non-exponential models were used to calculate tumor growth rate. Because these models have more than one variable, univariate analyses were performed and several mathematical models (that is, Logistic, Bertalanffy and Gompertz), which included the tumor growth limit variable, were optimized and fitted without any specific designation using the

Python `curve_fit` function. The univariate analyses result is presented in [Supplementary Table 1](#). The schematic workflow is illustrated in [Figure 1](#).

To validate the calculated  $\alpha$  by examining the correlation between  $\alpha$  and clinical variables including changing tumor size, primary tumor site, metastasis site, and number of metastasis lesions at baseline. The correlation between  $\alpha$  and changing tumor size and  $\alpha$  and number of metastases was analyzed using spearman correlation, while the other variables were analyzed using the Cramer's V correlation test. To test correlation, the primary cancer sites were classified into three categories: Cutaneous, Mucosal, and Ocular. Patients without primary site information were classified as Unknown. In addition, the study focuses on four major metastasis sites, namely the liver, lung, brain, and bone, and examines the correlation between alpha and each of these organs. For validate the interpretation of the Spearman and Cramer's V correlation coefficient, we followed the guidelines table in [Supplementary Table 6](#) which is based on we used Akoglu (10) and Kim's (11) guidelines.

## 2.5 Study outcomes

The primary study outcome was overall survival, which is defined as the time from ICB initiation to time of all-cause mortality. Secondary outcomes were (i) progression-free survival (PFS), defined as the time from treatment initiation to disease progression or death, whichever came first; (ii) PFS2, time to subsequent disease progression or death, whichever came first, after the next line of therapy; and (iii) percentage of tumor volume change at the first response evaluation ( $TP_{+1}$ ), defined as follows:

$$\begin{aligned} & \text{**Tumor volume change** (\%)} \\ & = \frac{V_{TP_{+1}} - V_{TP_{-0}}}{V_{TP_{-0}}} \times 100\% \end{aligned} \quad \text{Equation 2}$$

where  $V_{TP_{+1}}$  is the total tumor volume at the first treatment response evaluation and  $V_{TP_{-0}}$  is the total tumor volume at the baseline.

## 2.6 Statistical analysis

The Kaplan-Meier method was used to estimate patient's overall survival, as well as log-rank tests to assess significant differences in survival curves, with a significance level of  $P \leq 0.05$ . As the fitted pre-treatment tumor growth rate did not follow a normal distribution ([Supplementary Figure 1](#)), the cohort was divided into quartiles based on the interquartile range of  $\alpha$ , with the upper quartile value of  $\alpha = 0.076 \text{ days}^{-1}$  identified as the threshold for the high-risk group. The study outcomes were compared between the slow-paced ( $\leq$  threshold) and fast-paced ( $>$  threshold) groups. All the other possible pairs of quartiles were compared, and the results indicated that the fastest growing tumor group (Q4) was consistently and distinctly associated with lower

overall survival compared to that of Q1, Q3, or Q1-3 ([Supplementary Table 2](#)).

Endpoints were also be compared based on the number of metastases measured at the time pembrolizumab initiated (baseline,  $TP_0$ ), in accordance with the current definition of oligometastasis.

Sensitivity analyses were conducted by changing the tumor volume (0.1 cc to 0.01 cc or 1 cc) and interval from  $TP_0$  to  $TP_{-1}$  (-150 to -30 days). The analyses assessed whether the robustness of the results was dependent on the assumption that the tumor volume of patients who first presented with metastases without evidence of gross disease at  $TP_{-1}$  was 0.1 cc (number of imputed data points = 44/total number of data points = 86). We used a diameter of less than <1 cc as the minimal detectable volume, based on current CT imaging capabilities (12).  $P < 0.05$  was regarded significant. Python version 3.8.8 and log-rank test in lifelines (lifelines 0.27.1) library was used for statistical analyses.

TABLE 1 Patient characteristics.

Variables	Number of patients	%
<b>Sex</b>		
Male	47	54.7%
Female	39	45.3%
<b>Age</b>		
Median (IQR)	57(49-65)	
<b>BRAF mutation</b>		
No	58	67.4%
Yes	11	12.8%
Unknown	17	19.8%
<b>Treatment line</b>		
First line	62	72.1%
$\geq 2^{\text{nd}}$ line	24	27.9%
<b>Primary type</b>		
Mucosal	20	23.3%
Acral	13	15.1%
Non-CSD	37	43.0%
CSD	2	2.3%
Others	14	16.3%
<b>Metastasis site</b>		
Brain involvement	11	12.8%
Liver involvement	23	26.7%
Bone involvement	21	24.4%
Lung involvement	32	37.2%
Lymph node involvement	46	53.5%
Others	18	20.9%

CSD, chronic sun damage.

### 3 Results

Patient and tumor characteristics are listed in Table 1. A total of 372, 1049, 909, and 778 gross tumor volumes of all metastatic sites were 3D contoured at TP<sub>-1</sub> (86 patients), TP<sub>0</sub> (86 patients), TP<sub>+1</sub> (61 patients), and TP<sub>+2</sub> (43 patients), respectively. The median metastatic lesion number and the total volume of all metastatic sites were 1 (range 1-61) and 0.1 cc (range 0.1-508.2 cc), 7 (range 1-73) and 28.4 cc (range 0.4-1194.8 cc), 7 (range 1-117) and 35.6 cc (range 0.5-2319.4 cc), and 7 (range 1-157) and 63.2 cc (range 0.2-4147.1 cc), at TP<sub>-1</sub>, TP<sub>0</sub>, TP<sub>+1</sub>, and TP<sub>+2</sub>, respectively. Median time interval between TP<sub>-1</sub> and TP<sub>0</sub> was -90 days (range -363 to -6 days).

The pretreatment tumor growth rate ( $\alpha$ ,  $\times 10^{-2}$  days<sup>-1</sup>) was median 4.71 (range -0.62 to 44.1). The pretreatment tumor growth rates of the fastest (Q4) and the slowest (Q1) growing tumor group were median 9.6 (range 7.7 and 44.1) and 0.03 (range -0.62 and 0.12), respectively.

The present study reveals a robust correlation between the rate of tumor growth and the changing tumor size, as evidenced by high Spearman rank correlation coefficient,  $S_p$  ( $S_p = 0.78$ ,  $P = 0.03$ ). In addition, a moderately strong association was observed between tumor growth and number of metastasis lesion ( $S_p = 0.52$ ,  $P < .001$ ), while metastasis at liver, lung, and brain showed moderate significance (Creamer's  $V$  coefficient,  $S_c = 0.32$ , 0.25, and 0.31, respectively). Conversely, bone and primary tumor site exhibited weak interpretation in this regard. (Supplementary Figure 3, Table 4 and 5). The evaluation of best response as compared with tumor volume change at the first treatment response are illustrated in Figure 2C. A weak positive correlation was observed between the pretreatment tumor growth rate and treatment response at the first response evaluation (TP+1); however, the correlation disappeared at the final overall response evaluation (Figure 2A-C). Figure 3 shows the volumetric change over time, according to the pretreatment tumor growth rate (Figure 3A. TP<sub>-1</sub> to TP<sub>0</sub>, Figure 3B. TP<sub>0</sub> to TP<sub>+1</sub> and TP<sub>+2</sub>).

With a median follow up of 35 months, the 3-year OS, PFS, and PFS2 rates were 30%, 13%, and 16%, respectively. The slow-paced group had significantly higher OS (3-year, 35% vs 0%, log-rank test  $P = 0.001$ ), PFS (3-year, 15% vs 0%,  $P = 0.004$ ), and PFS2 (3-year, 16% vs 0%,  $P = 0.035$ ) than those of the fast-paced group (Figure 4A). These differences became more prominent in the subgroup of patients with >5 metastases (Figure 4). The median survival of each endpoint and number of metastasis subgroup are described in Supplementary Table 3.

Figures 5A-C show that the results maintain their robustness in the context of different assumptions of patients without tumor volume at TP<sub>-1</sub>. For example, the pretreatment tumor growth rate ( $\alpha$ ) continued to be significantly correlated with overall survival under the assumption of the imputation volume of 0.01 or 1.0 cc ( $P = .002$  and  $P = .039$ ).

### 4 Discussion

We propose pretreatment tumor growth rate as a novel prognostic marker for OS, PFS, and PFS2 in metastatic patients. In the cohort of patients who had median cumulative tumor volume of 28.4 cc (range 0.4 - 1195 cc) from median 7 (range 1 - 73) metastases on baseline

imaging, pretreatment growth rate was 4.71 (range -0.6 - 44.1;  $\times 10^{-2}$  days<sup>-1</sup>). Fast-paced tumor growth rate was associated with more frequent disease progression and dismal overall survival following ICB compared to that of the slow-paced tumor growth rate. In the subgroup of patients with fewer than five metastases, as demonstrated in Figure 4B, there was no statistically significant difference in growth rate between subgroups, except for overall survival. While this may suggest that tumor growth rate can be disregarded in treating patients with fewer metastases, the moderately strong correlation between tumor growth rate and number of metastases indicates that the absence of statistical difference could be attributed to the small size of the data. The key finding to emphasize is that the impact of tumor growth rate on prognosis is notably significant in the subgroup of patients with more than five metastases, suggesting the potential expansion of the Oligo-Metastatic Disease (OMD) definition beyond its traditional counting-based approach. Further investigation is necessary to confirm this hypothesis. However, if tumor growth rates are slow enough to enable all targets to be treated even in patients with numerous metastatic lesions using modern radiation oncology techniques, this could indicate potential benefits of curative treatment.

Several serial imaging studies have shown that pretreatment tumor growth rate is a reliable, independent prognostic factor in early-stage non-small cell lung cancer following SABR (13, 14). In a study of 160 patients with T1-2N0M0 lung cancer, the gross tumor volume of a single lesion at initial diagnostic CT, gross tumor volume of paired lesion at SABR planning CT, and time interval (in days) between diagnostic and planning CT were used to calculate tumor growth rate as follows:  $\ln(\text{GTV}_2/\text{GTV}_1)/\text{time interval in days}$  (14). The median tumor growth rate was 0.4 (range -2.0 - 6.1;  $\times 10^{-2}$  days<sup>-1</sup>), which was lower than that of stage IV disease in this study (median 1.62). However, surprisingly, there was a wide range of overlap between stage I and stage IV cancer. Faster-growing tumors ( $\geq$  median), compared to slower-growing tumors ( $<$  median), were associated with increased risk of regional recurrence and distant metastasis with decreased overall survival following SABR, which implies that tumor growth rate has a substantial clinical relevance in early-stage cancers.

Recent consensus proposed a comprehensive characterization of OMD based on dynamic OMD state model (15). In this context, it might be a reasonable option to consider repeated SABRs for selected patients with recurrent OMDs, as long-term survival following repeated ablative therapies was reported (16, 17). Recently, the post-local therapy disease pace was suggested as a major consideration before offering repeat local therapy in intracranial metastases (18) and extracranial metastases (19). In 107 patients with melanoma and brain metastases treated with stereotactic radiosurgery (18), faster tumor growth ( $>4$  cc/year) before repeat stereotactic radiosurgery was associated with a shorter time to second brain failure, increased need for salvage whole brain RT, and worse overall survival rate. In 303 patients with 1-5 extra-cranial metastases treated with SABR (19), the fast pace to second failure after first SABR was associated with subsequent widespread failure and reduced overall survival rate. Additionally, higher cumulative volume of metastases at baseline and oligo-progression/persistence type (vs. oligorecurrence) were associated with faster pace of metastases. In both studies (18, 19), tumor growth rate was calculated as the cumulative volume or numbers of new

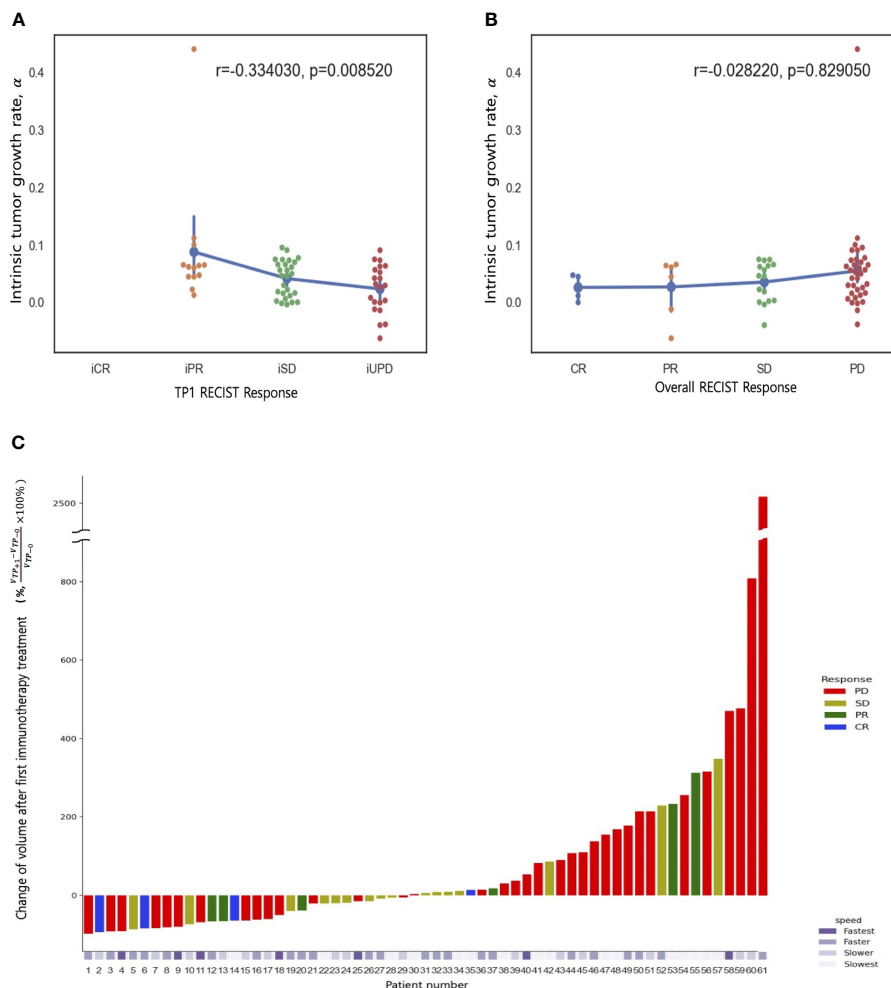


**FIGURE 2** Spearman rank correlation between tumor growth rate ( $\alpha$ ) and treatment response (A) at first response evaluation (TP<sub>+1</sub>) and (B) the best overall response (any time from the start of ICB treatment until disease progression). (C) A waterfall plot of percentage changes in tumor volume compared to measurements at baseline (TP<sub>0</sub>) according to the best overall response category. The bottom panel represents the pretreatment tumor growth rate ( $\alpha$ ).

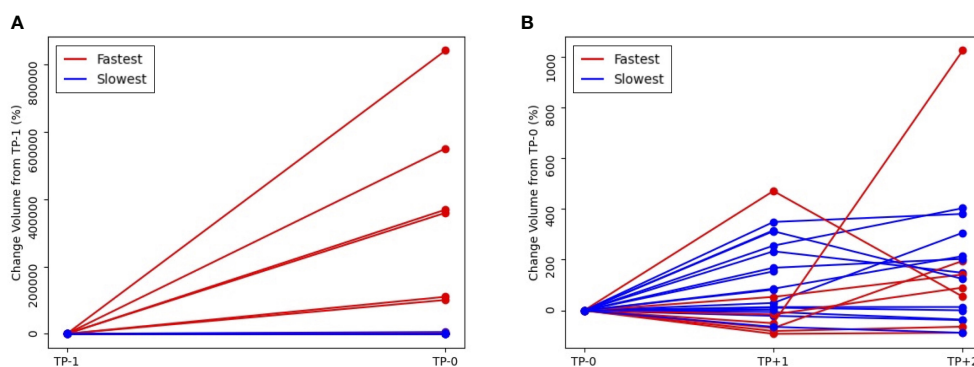


**FIGURE 3** Volumetric change of tumor volume over time, according to the pretreatment tumor growth rate (A) from pretreatment, TP<sub>-1</sub> to baseline, TP<sub>0</sub> and (B) from TP<sub>0</sub> to first response evaluation, TP<sub>+1</sub> and second response evaluation, TP<sub>+2</sub> (red line, fastest growing tumor group vs blue line, slowest growing tumor group).

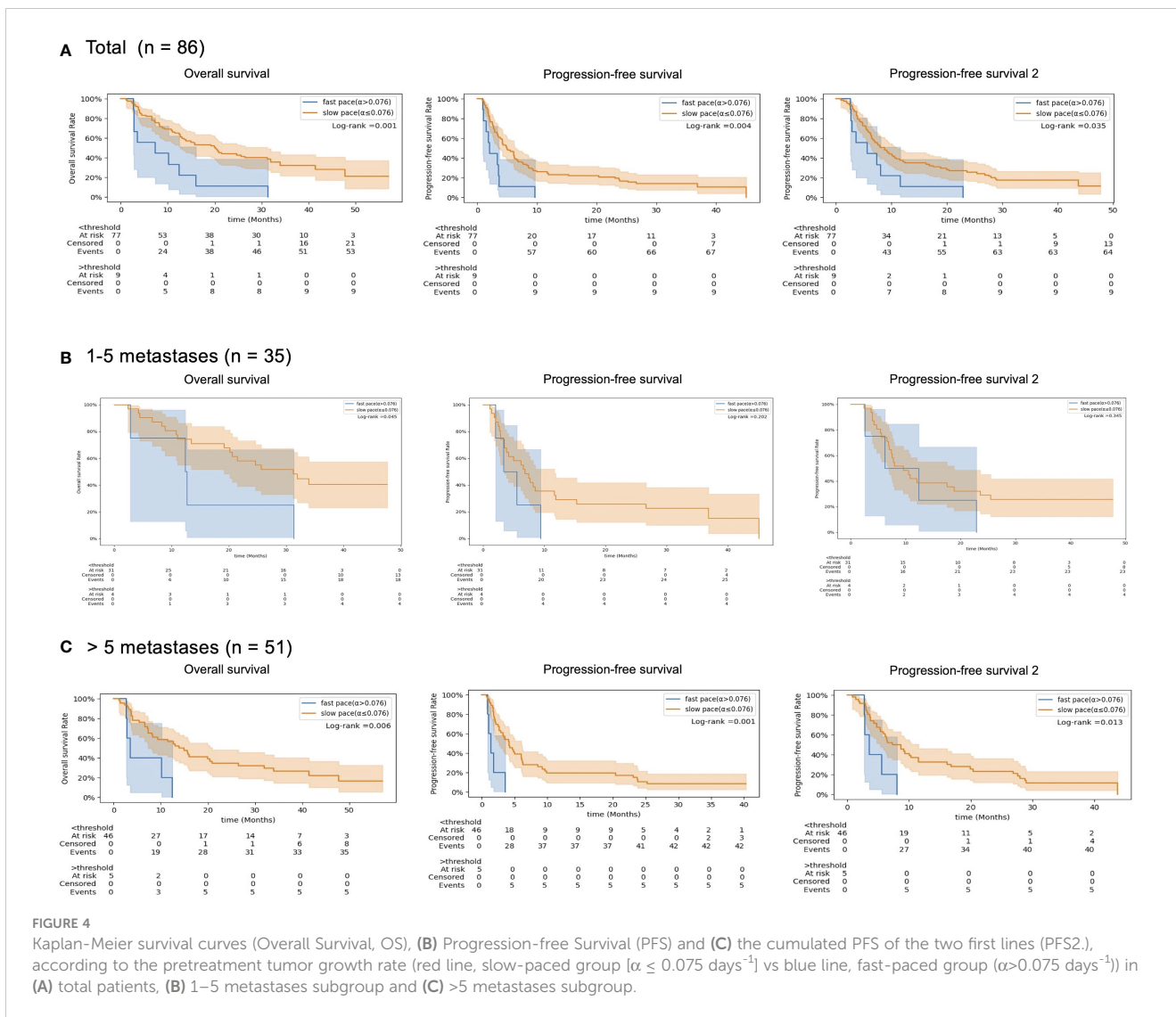


FIGURE 4

Kaplan-Meier survival curves (Overall Survival, OS), (B) Progression-free Survival (PFS) and (C) the cumulated PFS of the two first lines (PFS2), according to the pretreatment tumor growth rate (red line, slow-paced group [ $\alpha \leq 0.075 \text{ days}^{-1}$ ] vs blue line, fast-paced group ( $\alpha > 0.075 \text{ days}^{-1}$ )) in (A) total patients, (B) 1–5 metastases subgroup and (C) >5 metastases subgroup.

metastases divided by the time to subsequent failure. Collectively, we believe that tumor growth rate is a novel metric to differentiate actual OMDs from a transition phase to polymetastatic diseases.

This study had some limitations. Sample size, single ethnicity, and single histology suggest that the findings should be validated in independent datasets. In addition, we could not determine whether the ablation of all metastases in patients with slow tumor growth rate regardless of the number of metastatic lesions improved the overall survival rate. Due to the lack of a clinically established cut-off value for tumor growth rate, we use the definition of oligometastasis to identify the high-risk group. We have tested all possible combinations of quartile groups to avoid bias, and our results consistently demonstrate that the group with the fastest growing tumors (Q4) has lower overall survival compared to Q1, Q3, or Q1-3. However, if the threshold is changed to a lower quartile, the statistical difference between endpoints becomes difficult to identify (Supplementary figure 2). Further studies should determine the optimal methodological assessment of tumor growth rate and the appropriate cut-off point between oligometastasis and polymetastatic cancer.

The major strengths of this study include the manual contouring of 3,108 gross tumor volumes in patients with metastatic cancer, including polymetastatic cancers and OMDs in serial imaging and objective quantification of tumor growth rate using mathematical modeling. Mathematical modeling enables designing in-silico clinical trials that can guide the design of actual clinical trials (20–22). In this study, we began with a basic formulation of tumor growth to demonstrate its potential as an OMD biomarker. Other complexities such as metastatic locations or treatment modalities were not taken into account. They may be included in the future application but would also limit generalizability.

We have shown that pretreatment tumor growth rate in stage IV melanoma patients administered ICB can provide information on limited metastatic potential and possibility of long-term survival. In addition, it can help identify the oligometastatic patients most likely to benefit from local treatment within the capabilities of current treatment techniques. The advantage of tumor growth rate for OMD classification and in choosing appropriate treatment for the condition should be further investigated in prospective studies. Given that deep learning has shown its potential for auto-

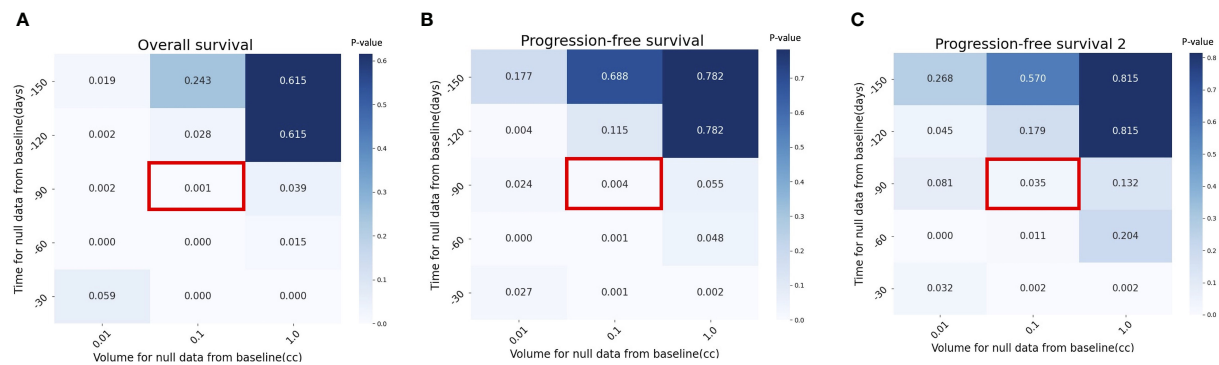


FIGURE 5

Sensitivity analysis with *p* value by different assumptions for null data at pretreatment, TP<sub>-1</sub> in (A) Overall Survival (OS), (B) Progression-Free Survival (PFS) and (C) cumulative PFS of the two first lines (PFS2). Red box indicates the assumption used in the current study (time for null data = -90 days and volume for null data = 0.1 cc).

contouring normal organs (23) in the whole body and gross tumor volumes (24) in localized disease, we are currently developing deep learning-based auto-segmentation of all potential metastatic lesions as a more time-efficient alternative than manual segmentation. The advantage of deep learning-based auto-segmentation of metastases is the possibility of quickly estimating the disease burden at each time point. Thereafter, the proposed mathematical modeling can be used to calculate the pretreatment tumor growth rate using the information of disease burden change in serial imaging. Collectively, these approaches have the potential to advance the field of OMDs by improving classification and patient selection not only at the time of diagnosis of metastasis but also during follow-up.

## Data availability statement

The raw data supporting the conclusions of this article will be made available by the authors, without undue reservation.

## Ethics statement

The studies involving human participants were reviewed and approved by Severance hospital's Institutional Review Board (4-2021-1683). Written informed consent for participation was not required for this study in accordance with the national legislation and the institutional requirements.

## Author contributions

Conceptualization: JC, WS. Formal analysis: YS, JC, WS. Resources: YS, JC, YK, SS, JK, TK, ML, RO, JSK, WS. Data curation: JC, JK, TK, JSK. Writing: YS, JC, WS. Review and

editing: ML, RO, JSK. Supervision: JC, WS. Project administration: JC, WS. All authors contributed to the article and approved the submitted version.

## Funding

This study was supported by a grant from the National Research Foundation of Korea (NRF) funded by the Korean Government (MSIT) [NRF-2021R1C1C1005930 and NRF-2022R1F1A1074344].

## Conflict of interest

The authors declare that the research was conducted in the absence of any commercial or financial relationships that could be construed as a potential conflict of interest.

## Publisher's note

All claims expressed in this article are solely those of the authors and do not necessarily represent those of their affiliated organizations, or those of the publisher, the editors and the reviewers. Any product that may be evaluated in this article, or claim that may be made by its manufacturer, is not guaranteed or endorsed by the publisher.

## Supplementary material

The Supplementary Material for this article can be found online at: <https://www.frontiersin.org/articles/10.3389/fonc.2023.1061881/full#supplementary-material>

## References

- Lang P, Gomez DR, Palma DA. Local ablative therapies in oligometastatic nsclc: new data and new directions. *Semin Respir Crit Care Med*. Thieme Medical Publishers (2020). 41(3):369-376. doi: 10.1055/s-0039-3400290
- Hellman S, Weichselbaum RR. Oligometastases. *J Clin Oncol* (1995) 13(1):8-10. doi: 10.1200/JCO.1995.13.1.8
- Olson R, Mathews L, Liu M, Schellenberg D, Mou B, Berrang T, et al. Stereotactic ablative radiotherapy for the comprehensive treatment of 1-3 oligometastatic tumors (Sabr-Comet-3): study protocol for a randomized phase iii trial. *BMC Cancer* (2020) 20(1):1-12. doi: 10.1186/s12885-020-06876-4
- Palma DA, Olson R, Harrow S, Correa RJ, Schneiders F, Haasbeek CJ, et al. Stereotactic ablative radiotherapy for the comprehensive treatment of 4-10 oligometastatic tumors (Sabr-Comet-10): study protocol for a randomized phase iii trial. *BMC Cancer* (2019) 19(1):1-15. doi: 10.1186/s12885-019-5977-6
- Rao A, Vapiwala N, Schaeffer EM, Ryan CJ. Oligometastatic prostate cancer: a shrinking subset or an opportunity for cure? *Am Soc Clin Oncol Educ Book* (2019) 39:309-20. doi: 10.1200/EDBK\_239041
- Palma DA, Olson R, Harrow S, Gaede S, Louie AV, Haasbeek C, et al. Stereotactic ablative radiotherapy for the comprehensive treatment of oligometastatic cancers: long-term results of the sabr-comet phase ii randomized trial. *J Clin Oncol* (2020) 38(25):2830. doi: 10.1200/JCO.20.00818
- Ottaiano A, Santorsola M, Caracò F, Caraglia M, Nasti G. Initial tumour burden and hidden oligometastatic disease in phase 3 clinical trials. *Lancet Oncol* (2022) 23(4):452-4. doi: 10.1016/S1470-2045(22)00034-1
- Kim J, Chang JS, Sung W, Kim JS, Kim TH, Choi SH, et al. A comparison of two disease burden assessment methods (3d volume versus the number of lesions) for prognostication of survival in metastatic melanoma: implications for the characterization of oligometastatic disease. *Int J Radiat Oncol Biol Phys* (2022). 114(5):883-891. doi: 10.1016/j.ijrobp.2022.08.040
- Murphy H, Jaafari H, Dobrovolsky HM. Differences in predictions of ode models of tumor growth: a cautionary example. *BMC Cancer* (2016) 16(1):1-10. doi: 10.1186/s12885-016-2164-x
- Akoglu H. User's guide to correlation coefficients. *Turkish J Emergency Med* (2018) 18(3):91-3. doi: 10.1016/j.tjem.2018.08.001
- Kim H-Y. Statistical notes for clinical researchers: chi-squared test and fisher's exact test. *Restorative Dentistry Endodontics* (2017) 42(2):152-5. doi: 10.5395/rde.2017.42.2.152
- Winer-Muram HT, Jennings SG, Tarver RD, Aisen AM, Tann M, Conces DJ, et al. Volumetric growth rate of stage I lung cancer prior to treatment: serial ct scanning. *Radiology* (2002) 223(3):798-805. doi: 10.1148/radiol.2233011026
- Atallah S, Le LW, Bezjak A, MacRae R, Hope AJ, Pantarotto J. Validating impact of pretreatment tumor growth rate on outcome of early-stage lung cancer treated with stereotactic body radiation therapy. *Thorac Cancer* (2021) 12(2):201-9. doi: 10.1111/1759-7714.13744
- Atallah S, Cho BJ, Allibhai Z, Taremi M, Giuliani M, Le LW, et al. Impact of pretreatment tumor growth rate on outcome of early-stage lung cancer treated with stereotactic body radiation therapy. *Int J Radiat Oncol Biol Phys* (2014) 89(3):532-8. doi: 10.1016/j.ijrobp.2014.03.003
- Guckenberger M, Lievens Y, Bouma AB, Collette L, Dekker A, Nandita MD, et al. Characterisation and classification of oligometastatic disease: a European society for radiotherapy and oncology and European organisation for research and treatment of cancer consensus recommendation. *Lancet Oncol* (2020) 21(1):e18-28. doi: 10.1016/S1470-2045(19)30718-1
- Taylor C, Correa C, Duane FK, Aznar MC, Anderson SJ, Bergh J, et al. Estimating the risks of breast cancer radiotherapy: evidence from modern radiation doses to the lungs and heart and from previous randomized trials. *J Clin Oncol* (2017) 35(15):1641-9. doi: 10.1200/JCO.2016.72.0722
- Harrow S, Palma DA, Olson R, Gaede S, Louie AV, Haasbeek C, et al. Stereotactic radiation for the comprehensive treatment of oligometastases (Sabr-Comet)-extended long-term outcomes. *Int J Radiat Oncol Biol Phys* (2022). 114(4):611-616. doi: 10.1016/j.ijrobp.2022.05.004
- LeCompte MC, McTyre E, Henson A, Farris M, Okoukoni C, Cramer CK, et al. Survival and failure outcomes predicted by brain metastasis volumetric kinetics in melanoma patients following upfront treatment with stereotactic radiosurgery alone. *Cureus* (2017) 9(12):e1934. doi: 10.7759/cureus.1934
- Willmann J, Badra EV, Adilovic S, Christ SM, Ahmadsei M, Mayinger M, et al. Distant metastasis velocity as a novel prognostic score for overall survival after disease progression following stereotactic body radiotherapy for oligometastatic disease. *Int J Radiat Oncol Biol Phys* (2022). (2022). 114(5):871-882. doi: 10.1016/j.ijrobp.2022.06.064
- Sung W, Hong TS, Poznansky MC, Paganetti H, Grassberger C. Mathematical modeling to simulate the effect of adding radiation therapy to immunotherapy and application to hepatocellular carcinoma. *Int J Radiat Oncol Biol Phys* (2022) 112(4):1055-62. doi: 10.1016/j.ijrobp.2021.11.008
- McClatchy DM, Willers H, Hata AN, Piotrowska Z, Sequist LV, Paganetti H, et al. Modeling resistance and recurrence patterns of combined targeted-chemoradiotherapy predicts benefit of shorter induction period. *Cancer Res* (2020) 80(22):5121-33. doi: 10.1158/0008-5472.CAN-19-3883
- Scarborough JA, Tom MC, Kattan MW, Scott JG. Revisiting a null hypothesis: exploring the parameters of oligometastasis treatment. *Int J Radiat Oncol Biol Phys* (2021) 110(2):371-81. doi: 10.1016/j.ijrobp.2020.12.044
- Choi MS, Choi BS, Chung SY, Kim N, Chun J, Kim YB, et al. Clinical evaluation of atlas-and deep learning-based automatic segmentation of multiple organs and clinical target volumes for breast cancer. *Radiother Oncol* (2020) 153:139-45. doi: 10.1016/j.radonc.2020.09.045
- Primakov SP, Ibrahim A, van Timmeren JE, Wu G, Keek SA, Beuque M, et al. Automated detection and segmentation of non-small cell lung cancer computed tomography images. *Nat Commun* (2022) 13(1):1-12. doi: 10.1038/s41467-022-30841-3